Diagnosis of fault brush winding stator induction motor using external sensor flux of three axes

Rezi Delfianti[1], Yusrizal Afif[1], Fidya Eka Prahesti[2], Bima Mustaqim[3], Bolas Boy Silalahi[4]
[1]Department of Electrical Engineering, Faculty of Advanced Technology and Multidiscipline, Airlangga University, Surabaya, Indonesia
[2]Faculty of Engineering, Nusantara PGRI Kediri University, Kediri, Indonesia
[3]Department of Educational Technology, Faculty of Education, Universitas Negeri Medan, Medan, Indonesia
[4]Department of Electrical Engineering, Faculty of Intelligent Electrical and Informatics Technology,
Institut Teknologi Sepuluh Nopember, Surabaya, Indonesia

Article Info

ABSTRACT

This research investigates short-circuit problems in induction motor stators by constructing a motor with a changing winding and leaking flux data. The data is used to evaluate X, Y, and Z axes and map motor waves under normal and abnormal conditions. This study is expected to compare the effectiveness of the observation method from three different axes at the same motor condition to be further helpful in repairing induction motor damage caused by the circuit. From the results of the study, it shows that the harmonic value of the stator current will be more effective than the Y axis with a harmonic amplitude value of -38.8 dB, higher than the harmonic value of the current on the X axis with a difference of 33.89 dB and a difference of 0.32 dB from the Z axis. Suppose the disturbance is measured from the stray harmonic value. In that case, the flux will be more effective than the X axis with a harmonic amplitude value - 25.27 dB, higher than the harmonic value of the flux on the Y axis with a difference of 6.425 and a difference of 4.85 dB from the Z axis.

Corresponding Author:

Rezi Delfianti
Department Electrical Engineering, Faculty of Advanced Technology and Multidiscipline,
Airlangga University
Campus C, St. Dr. Ir. H. Soekarno, Mulyorejo 60115, Surabaya, East Java, Indonesia
Email: rezi.delfianti@ftmm.unair.ac.id

1. INTRODUCTION

An AC motor that operates by generating induction voltage through the magnetic field created by the stator is referred to as an induction motor [1]. The induction motor is a well-known piece of machinery employed in various industrial domains. Hence, it is essential to monitor and identify any disruptions in this rotating motor to ensure the safety, effectiveness, and optimal operation of induction motors [2]. There are four types of disturbances that may manifest in the motor: electrical disruptions, mechanical issues, bearing problems, and interference caused by motor lubrication [3], [4]. A prevalent issue observed in induction motors is electrical disturbance, frequently arising from short-circuits that impact the windings of the stator coil [5]. Since this condition is not visible to the naked eye, it is challenging to identify [6].

The onset of this disruption arises from an insulation breakdown between the windings, resulting in a short circuit [7]. Alternatively, the occurrence of an arc flash on the windings can also give rise to this short circuit in some instances [8]. Impairment to the stator winding can lead to irregularities in the rotation of the induction motor, resulting in an asymmetrical current in the stator. This asymmetry causes an imbalance in the generated flux. Such a flux alteration can serve as an indicator for detecting short-circuit disturbances in

the stator winding of the induction motor [9]. In stator windings, usually, the stator windings consist of sufficient insulation thickness and multiple sparks are also generated means that insulation will survive, so winding short circuit will happen between winding in worst conditions only [10].

In earlier research on identifying stator short circuits, numerous studies employed the technique of analyzing stator current, which is also referred to as motor current spectrum analysis (MCSA) [11]. This approach is utilized to examine the frequency spectrum attributes of the stator current. It is a preferred method due to its simplicity of application and cost-effectiveness, as it does not demand significant expenses [12].

However, certain research endeavors have devised alternative techniques for identifying disruptions within the induction motor. The utilization of external sensor flux for magnetic field analysis has gained popularity, primarily due to its simplicity in implementation and its capability for non-invasive diagnosis [13]. In their research, some scientists have employed stray flux analysis techniques, including the identification of motor rotor malfunction in motors and the detection of short circuits in the stator winding [14]. Analysis of bearing damage [15], Analysis of motor air gap eccentricity [16], and numerous additional methods. In an earlier investigation focused on identifying short-circuit faults in the stator winding, they pinpointed induction motors displaying signs of stator issues [11]. However, the majority employ a single-directional sensor coil, concentrating solely on the flux quantity from either the X-axis or the Y-axis (2D). In this research, we will examine the detection of short-circuit faults in the stator winding of an induction motor by employing a flux spectrum approach with a lower sampling frequency and coil sensors capable of capturing signals from three dimensions (3D), namely the X-axis, Y-axis, and Z-axis. Subsequently, the obtained outcomes will be analyzed and compared with the motor current spectrum analysis (MCSA) technique to determine if utilizing stray flux signals yields greater sensitivity compared to stator currents [17].

2. BASIC THEORY
2.1. Three-phase induction motor

The operational principle of an induction motor relies on the induction of a magnetic field. When current flows through the stator, it induces a rotating magnetic field, which in turn generates flux and sets the rotor into motion [18]. Achieving equilibrium in the current passing through the stator will produce a balanced flux [19]. Nevertheless, if there is a disruption in the stator winding, like a short circuit, it will result in an uneven current distribution, leading to an asymmetrical flux, which in turn gives rise to stray flux emanating around the motor [20].

The rotor's speed consistently converges toward the rotating field since the flux created on the rotor lags behind the flux on the stator [21]. The speed of the rotating field is referred to as synchronous speed, which is determined by the number of poles (p) in the induction motor, as (1).

$$n_1 = \frac{120.fs}{p} \tag{1}$$

Regarding the rotor field, it exhibits a lagging or slower speed compared to the stator.

$$n = n_1 - \frac{120.fs}{p} \tag{2}$$

The variance between synchronous speed and rotor speed is termed motor slip. Consequently, motor slip can be expressed as (3).

$$S = \frac{n_1 - n}{n_1} \times 100\% \tag{3}$$

Where S = motor slip, n_1 = synchronous speed (stator field speed), and n = speed of the rotor field.

Synchronous speed is contingent upon both the quantity of motor poles and the frequency of the supplied voltage [22]. The rotor field velocity, on the other hand, hinges on both synchronous speed and the motor's workload. Increased motor load results in greater slip and a decrease in rotor speed. The rotor constitutes the rotating component of the motor, whereas the stator remains stationary, housing numerous windings capable of inducing a magnetic field. Measuring rotor speed is essential for slip calculations in determining the frequency components that influence stator short-circuit disturbances [23]. Induction motors consist of two primary elements, depicted in Figure 1 the rotor and the stator. The rotor is the component that rotates, while the stator remains fixed in place. Within the stator, multiple windings are capable of generating a magnetic field [24].

Figure 1. The three-phase induction motor and its components

2.2. Short circuit

Short circuit interference can be caused by an insulation failure in the stator winding of the induction motor [25]. Short circuit interference generally begins with partial discharge caused by physical factors of a defective motor and external factors. A short circuit can occur between two coils of the same phase, between phases, and between phases and ground [11].

Generally, the occurrence of short circuits in induction motors begins with a decrease in the insulation strength of the motor stator windings [26]. A temporary short course and a small current occur quickly because the insulation impedance is still high. Temporary short circuits occur non-periodically because the insulation of the motor stator windings is still quite strong. Short circuits will still occur if there is no improvement to the insulation of the motor stator winding. Still, it only lasts temporarily, after which the motor will continue to operate as usual [10].

2.3. Flux on 3 phase induction motor

In induction motor 3 phase, when there are three coils that shift 120 degrees electricity in the room and given a voltage that shifts 120° With respect to time (three phases), the resultant flux will be embossed and as if there were magnetic poles that mechanically rotated [27]. Stray flux refers to a magnetic flux emitted from within the engine enclosure, and it is directly associated with the magnetic motor [28]. Stray flux is generated due to variations in the spectral components of stator and rotor currents. An initial conjecture suggests that stray flux emerges from the component labeled as "0" of the primary flux of the induction motor, which relates to the static reference section while the reference section itself rotates [29].

2.4. Motor current signature analysis

Motor current signature analysis (MCSA) is a method that is often used to detect short-circuit disturbances in induction motors [3]. This method is widely used because it can be used without affecting the motor's performance in operation. This method is also simple and economical in detecting disturbances in the motor. In detecting interference, an electrical signal is used that is contained in the stator current while it is operating [30]. The obtained stator current spectrum will be converted into a frequency domain to find the point of fault using Fourier transform [9]. In its application, interference caused by damage to the insulation failure of the stator winding can be observed through abnormal harmonic frequencies. The equation can know abnormal harmonic frequencies:

$$f\ stator\ =\ fs\ [n\,(1-s)\ \pm\ k] \tag{4}$$

2.5. Harmonics arising from stator internal-turn short circuit fault

The presence of a short circuit in the stator winding can be detected by monitoring unusual harmonic frequencies [31], [11]. The equations such as the one below can help identify unusual harmonic frequencies derived from the current spectrum:

$$f_{stator} = f_s \left[\frac{n}{p}.(1-s) \pm k) \right] \tag{5}$$

Where f_{stator} = forecasting the frequency associated with stator winding damage, n = integer (1,2,3, ...), k = integer constant (1,3,5 ...), p = pairs of poles, and f_s = the frequency of the power supply.

2.6. Fast Fourier transform (FFT)

Fast Fourier transform (FFT) is an algorithm to calculate discrete Fourier transform (DFT) more quickly and efficiently. FFT is often used to present signals in discrete time domains and frequencies. The advantage of using FFT is that it reduces the complexity of transformations that DFT performs faster. FFT is often applied to process digital signals or solve partial differential equations into algorithms for integer doubling [32]. The fundamental difference in DFT computational load is quite heavy because it requires

several N2 complex multiplications, while FFT has a lighter computational load [33]. The FFT will divide the sampling results into several parts, which will then be solved using the same algorithm and collected back into one part. The Fourier transform presents a continuous spectrum of nonperiodic signals. The Fourier X(f) transformation of the constant time x(t) is (6).

$$X(f) = \int_{-\infty}^{\infty} x(t)e^{-i\omega t}$$

(6)

The transformation inverse is (7).

$$X(t) = \int_{-\infty}^{\infty} x(f)e^{-i\omega t}$$

(7)

Where: $X(f)$ = signal in the frequency domain, $X(t)$ = signal in the time domain, $x(t)e^{-i\omega t}$ = constant value of a time domain signal, $x(f)e^{-i\omega t}$ = constant value of a frequency domain signal, f = frequency, and t = time. The Fourier transform can process signals such as current, stator voltage, stray flux, noise, speed, temperature, and shaft vibration.

3.   THE ROLE OF THE SYSTEM

This chapter will explain how to start a motor fault detection research experiment on the stator. System configuration is the initial stage in this study after that goes into the section on how the researcher method of data collection. After all the required data has been completed, enter the following stage, namely the data acquisition process using MATLAB and VIEW lab.

3.1. Configuration system

The research aimed to detect disturbances in 3-phase induction motors resulting from insulation failures in the motor stator windings, employing the analysis methods of stray flux spectrum and stator current spectrum. During the experiments, an AC voltage power source with a capacity of 1500 Watts was utilized to drive the 3-phase induction motor. Mechanical loading was applied through the coupling of the induction motor shaft with a 3-phase synchronous generator, while electrical loading was achieved by connecting the motor to an incandescent lamp circuit, powered by a 3-phase synchronous generator. Various configurations and gear setups were explored throughout the experimental process.

Experimental data retrieval involves the use of several tools, such as laptops equipped with LabVIEW, Diadem, Excel, and MATLAB software. Additionally, NI DAQ 9246 is utilized for acquiring stator current measurement data, and NI DAQ 9775 is employed to collect flux stray measurement data. Establishing a connection between NI DAQ 9246 and NI DAQ 9775 with LabVIEW software is crucial prior to commencing the experiment. Following data acquisition, the information gathered during the investigation will be processed using Diadem, Excel, and MATLAB software, leveraging the fast Fourier transform (FFT) method for in-depth analysis.

The motor used in this experiment is a 3-phase induction motor of a squirrel cage with a capacity of 2 HP with several 4 poles. The motor has a voltage rating of 220/380 Volts and a current rating of 3.68/6.36 A with a Wye (Y) winding configuration. The motor's synchronous speed is 1500 rpm at no-load and 1400 rpm at full-load conditions. This experiment used a 3-phase synchronous generator as a system load. The generator will supply power to the incandescent lamp circuit as an electrical load that can be configured according to the required data. The induction motor will be coupled with a synchronous generator to generate power that will supply the incandescent lamp circuit. The experiment was conducted with normal and short-circuit motor conditions. The investigation will be carried out starting from the time of the motor without load, the motor with a load of 25%, the motor with a load of 50%, and a load of 100%. The purpose of the load is to determine the impact of the experimental results more visibly specific. The loading system in this experiment used an incandescent lamp circuit with a total load close to 1500 W at the time of maximum load (100%), and the nominal current of the induction motor reached 3.68 A, as in Figure 2.

3.2. Data retrieval

To ensure precise data collection, a thorough system configuration process precedes the initiation of the data retrieval procedure. This comprehensive setup encompasses several critical steps' Measurement: The system includes the measurement of the motor's rotational speed (rpm) using a tachometer. While the motor is in operation, the tachometer is equipped with a sensor placed near the motor shaft's end to detect its rotation and calculate the rpm accurately. Stray flux capture: Gauss meter sensors are strategically positioned near the motor to effectively capture stray flux signals. This Gauss meter operates on the induction principle, featuring an induced coil and a measuring instrument. Fluctuations in flux density within the coil lead to changes in electrical energy, resulting in the generation of inductance and a magnetic field. The Gauss meter

detects the force produced by the rotating coil, collecting data from three different axes during each experiment. Gauss meter adjustment: Before the commencement of the investigation, precise adjustments are made to the Gauss meter. This aligns the coil with the intended data collection direction: parallel to the motor shaft for X-axis data, perpendicular to the motor shaft for Y-axis data, and transversely against the motor shaft for Z-axis data, ensuring accurate measurements from various orientations.

Additionally, the power quality and Fluke motor analyzer are utilized to detect stator current anomalies, such as short circuit faults in the motor. This versatile instrument is capable of measuring various electrical parameters, including voltage, frequency, current, complex power, active power, reactive power, and power factor. The experimental circuit is configured using LabVIEW software in conjunction with the NI 9246 tool, which captures current signals during steady-state motor conditions. Meanwhile, flux sensors equipped with the IDR-210 Gauss meter capture the flux signal, enhancing the comprehensive data acquisition process.

3.3. Data acquisition process

The data retrieval process is meticulously organized, beginning with a well-planned series of experiments. Initially, experiments are conducted under normal motor conditions, without any load, to measure both current and stray flux. This phase of investigation is carried out twice, gathering data from the Y and Z axes, while data for the X-axis is drawn from existing records. Following this, the motor is connected to a 3-phase generator for experiments under normal motor conditions, but with varying load levels set at 25%, 50%, 75%, and 100%. Each load variation yields data for both current and stray flux across three distinct axes. Upon collecting all the data under normal motor conditions, modifications are made to the R phase winding of the motor to introduce a short circuit fault. This involves creating tapping slots within one of the winding slots to facilitate short-circuit reconstruction. The subsequent experiment covers three variations of short circuit disturbances: inter-turn short circuit with 2 windings (SC1), inter-turn short circuit with 4 windings (SC2), and inter-turn short circuit with 8 windings (SC3), all applied to the R phase winding, as in Figure 3.

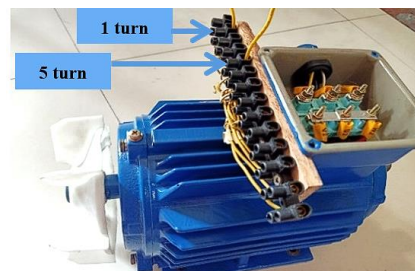Figure 2. Incandescent lamp circuit as a load

Figure 3. Configuration short inter turn short circuit 4 windings

This study will acquire the data using NI DAQ 9246 with the current sensor and NI DAQ 9775 with a Gauss meter sensor directly connected to LabVIEW software on laptops. The LabVIEW software will display stator current data read by NI DAQ 9246 and voltage signals from Gauss meters read by NI DAQ 9775 and then be acquired. The test result data in a technical data management streaming (tdms) file will be converted into a file xls using Diadem. The xls file can be read in detail using Microsoft Excel software. The files.xls will then be processed and analyzed using MATLAB software to obtain harmonic amplitude frequency values from each axis's stator current and flux stray. The harmonic value obtained will be compared using a diagram.

3.4. Data processing

In the experimental data collection process, a high sampling rate of 5000 Hz/s is employed, resulting in the acquisition of 50,000 sampling data points every second. This elevated sampling rate enhances data accuracy and simplifies subsequent data analysis, providing a more detailed representation of frequency components around the fundamentals when transformed into the time domain. To measure current and voltage signals, LabVIEW software is utilized, featuring both front panels and block diagrams. The front panel serves as the primary interface for creating virtual instruments, while the block diagram is employed for controlling the output of objects from the front panel.

Subsequently, the stator current and sensor output voltage signals are processed using diadem software. The data in the time domain is converted into the frequency domain using the fast Fourier transform (FFT) algorithm. This approach aids in diagnosing the presence of short circuit faults by analyzing

the spectra of stator current and stray flux. The results obtained from FFT are converted into xls format for further processing using MATLAB software, allowing the data to be represented in decibel units (dB). These decibel-based data sets are then compared across different axes through graphical diagrams, revealing variations in harmonic values across the three axes.

4.   DATA ANALYSIS
4.1. Interference frequency analysis
After obtaining the necessary data, a frequency analysis will be carried out on the current signal and flux stray to map the points of interference frequency, which can then be compared between the three axes. The analysis focused on two motor conditions: when the motor is in average condition and when the motor is in short circuit condition eight windings. Eleven interference frequency points are plotted for each data as in Table 1. The frequency points plotted to include 25 Hz, 50 Hz, 75 Hz, 100 Hz, 150 Hz, 200 Hz, 250 Hz, 300 Hz, 350 Hz, 400 Hz, and 450 Hz with a margin of ±3Hz.

4.2. Comparison of harmonic frequency amplitude values
The amplitude values obtained from 11 frequency points in each experimental data are averaged to make it easier to read the data and can henceforth be compared using diagrams. Comparison of harmonic frequency amplitude values, as in Table 1. After processing the data with MATLAB and obtaining the amplitude values for specified frequency points, the data will be visualized using a bar chart. This chart helps visualize the differences in amplitude values across all three axes for the 11 frequency points. By averaging the harmonic amplitude values for these points, a comparative analysis is performed. This analysis reveals that the amplitude values measured by the sensor exhibit variations across different axes, indicating differences in the sensor's sensitivity in capturing both stray flux signals and stator current on each axis. For instance, the average harmonic amplitude of current during normal motor operation without a load is -73.99 dB on the X-axis, -37.7 dB on the Y-axis, and -37.18 dB on the Z-axis. This significant difference suggests that the measurement of harmonic amplitude for current on the X-axis is notably lower than that on the Y and Z axes, implying that the measurement of current harmonic amplitude is more precise from the Y and Z axes compared to the X-axis.

Table 1. Average flux harmonic amplitude values (dB)

	N 0%	N 50%	N 100%	SC2 0%	SC2 50%	SC2 100%
Sb X	-73.99	-74.09	-74.06	-73.68	-73.08	-73.33
Sb Y	-37.7	-38.54	-39.88	-37.94	-39.32	-39.16
Sb Z	-37.18	-39.35	-41.63	-39.63	-37.17	-39.59
	SC4 0%	SC4 50%	SC4 100%	SC8 0%	SC8 50%	SC8 100%
Sb X	-73.41	-70.94	-73.57	-69.97	-70.31	-71.87
Sb Y	-37.71	-37.75	-40.19	-38.82	-39.86	-38.75
Sb Z	-38.81	-38.76	-40.78	-38.73	-38.45	-39.33
	N 0%	N 50%	N 100%	SC2 0%	SC2 50%	SC2 100%
Sb X	-25.69	-26.49	-26.61	-29.99	-25.47	-25.97
Sb Y	-33.7	-30.78	-31.02	-30.47	-30.35	-28.77
Sb Z	-31	-32.01	-32.52	-30.24	-30.81	-31.91
	SC4 0%	SC4 50%	SC4 100%	SC8 0%	SC8 50%	SC8 100%
Sb X	-24.84	-16.16	-26.4	-24.95	-24.99	-25.66
Sb Y	-31.27	-26.43	-28.92	-30.74	-29.59	-48.28
Sb Z	-29.62	-28.38	-28.9	-29.39	-28.32	-28.37

The average harmonic amplitude values for flux exhibit significant variations when compared to the average values of harmonic amplitude for current. For instance, under normal motor conditions without any load, the average harmonic amplitude of flux is -25.69 dB on the X-axis, -33.7 dB on the Y-axis, and -31 dB on the Z-axis. These differences in harmonic amplitude values for flux are more pronounced than the differences in harmonic amplitude values for current. Among the harmonic amplitude values for flux at the specified 11 frequency points, the amplitude on the X-axis consistently surpasses that on the Y and Z axes across all experimental conditions. Moreover, the differences in harmonic amplitude values for flux between the Y and Z axes are smaller compared to the differences between the X-axis and either the Y or Z axis. This implies that in the context of flux harmonic analysis, the data collection results indicate that measurements on the X-axis are more sensitive than those on the Y and Z axes.

Suppose the average value of the harmonic amplitude of current from all motor conditions and loading is averaged again, as in Figures 4 and 5. In that case, the harmonic amplitude of the current is -72.69 dB on the X-axis, -38.8 dB on the Y-axis, and -39.12 dB on the Z-axis. The current harmonic

amplitude value is highest on the Y axis, with a difference of 33.89 dB from the X axis and a difference of 0.32 dB from the Z axis. If the average value of the flux harmonic amplitude of all motor and loading conditions is averaged again, obtained the current harmonic amplitude value of -25.27 dB on the X axis, -31.69 dB on the Y axis, and -30.12 dB on the Z axis. From the measurement results, it is obtained to detect this motor disturbance using current harmonics will be more effective. Because the value obtained on the Y axis is more sensitive than the x and z axis.
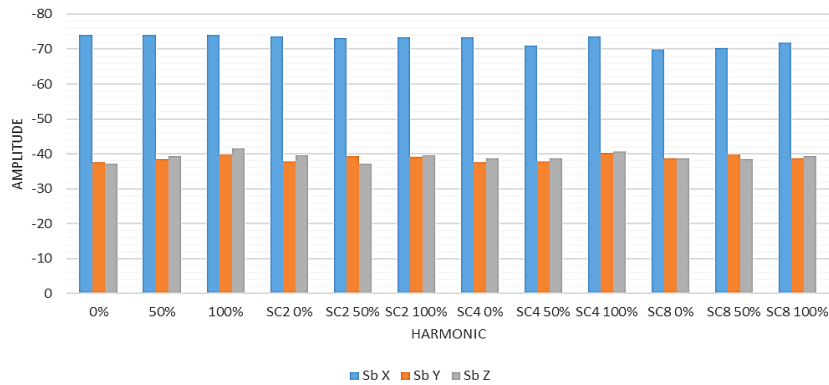
Figure 4. Diagram of the average value of the current harmonic amplitude of all motor and loading conditions
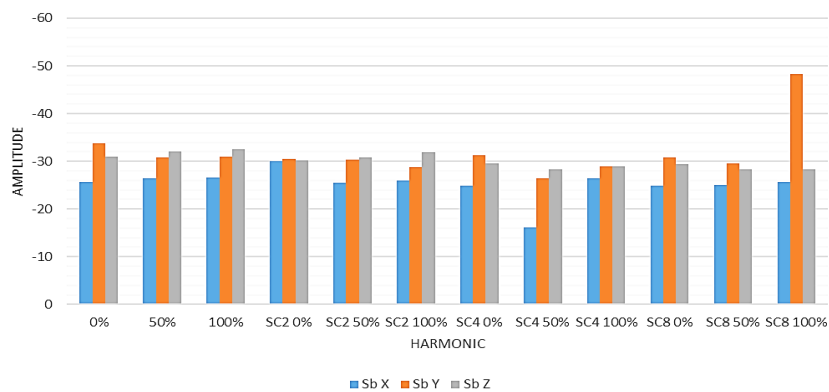
Figure 5. Diagram of the average value of the flux harmonic amplitude of all motor and loading conditions

5.   CONCLUSION

Based on the results of the analysis of experimental data that has been carried out in this final project, it can be concluded: i) The experimental data showed that the observation system successfully detected interference using FFT on the stator current signal and leaking flux, ii) Suppose the interference is measured from the stray harmonic value. Based on the average harmonic amplitude value obtained, detecting short circuit disturbances in a 3-phase induction motor by measuring from the harmonic value of the stator current will be more effective than the Y axis with a harmonic amplitude value of -38.8 dB, higher than the current harmonic value on the X axis with a difference of 33.89 dB and a difference of 0.32 dB from the Z axis. In that case, the flux will be more effective than the X axis with the harmonic amplitude value - 25.27 dB, higher than the harmonic value of the change on the Y axis with a difference of 6.425 and a difference of 4.85 dB from the Z axis.

REFERENCES

[1]   Y. Wang, W. Song, M. Yazdani-Asrami, and J. Fang, "A Fast Numerical Modeling Approach Based on Boundary Field Method for Calculating AC Losses in Superconducting Motors," *IEEE Transactions on Applied Superconductivity*, vol. 33, no. 3, pp. 1–6, Apr. 2023, doi: 10.1109/TASC.2023.3245039.

[2]   H. Henao *et al.*, "Trends in Fault Diagnosis for Electrical Machines: A Review of Diagnostic Techniques," *IEEE Industrial Electronics Magazine*, vol. 8, no. 2, pp. 31–42, Jun. 2014, doi: 10.1109/MIE.2013.2287651.

[3]   R. N. Dash, S. Sahu, C. K. Panigrahi, and B. Subudhi, "Condition monitoring of induction motors: — A review," in *2016 International Conference on Signal Processing, Communication, Power and Embedded System (SCOPES)*, Oct. 2016, pp. 2006–2011. doi: 10.1109/SCOPES.2016.7955800.

[4]   J. Penman, H. . Sedding, and ., "Detection and Location of Interturn Short Circuits," *IEEE Transactions on Energy Conversion*,

vol. 9, no. 4, pp. 652–658, 1994.

[5]   N. Wang, W. Zhao, M. Li, and X. Wang, "Design and Analysis of a Double-Stator Permanent Magnet Linear Motor Using Single-Sided Phase-Group Concentrated-Coil Windings," in *2022 25th International Conference on Electrical Machines and Systems (ICEMS)*, Nov. 2022, pp. 1–5. doi: 10.1109/ICEMS56177.2022.9983292.

[6]   L. Szabo, K. Biro, D. Fodor, and E. Kovács, "Improved Condition Monitoring System for Induction Machines Using a Model-Based Fault Detection Approach," 2006. [Online]. Available: https://www.researchgate.net/publication/229001975_Improved_Condition_Monitoring_System_for_Induction_Machines_Using_a_Model-Based_Fault_Detection_Approach

[7]   Z. Anthony, E. Erhaneli, Y. Warmi, Z. Zulkarnaini, A. Anugrah, and S. Bandri, "A new windings design for improving single-phase induction motor performance," *International Journal of Electrical and Computer Engineering (IJECE)*, vol. 12, no. 6, p. 5789, Dec. 2022, doi: 10.11591/ijece.v12i6.pp5789-5798.

[8]   S. A. Saleh, A. S. Aljankawey, R. Errouissi, and E. Castillo-Guerra, "Extracting the phase of fault currents: A new approach for identifying arc flash faults," in *2015 IEEE/IAS 51st Industrial & Commercial Power Systems Technical Conference (I&CPS)*, May 2015, pp. 1–10. doi: 10.1109/ICPS.2015.7266437.

[9]   A. Yazidi, H. Henao, G. A. Capolino, M. Artioli, F. Filippetti, and D. Casadei, "Flux signature analysis: An alternative method for the fault diagnosis of induction machines," in *2005 IEEE Russia Power Tech*, Jun. 2005, pp. 1–6. doi: 10.1109/PTC.2005.4524578.

[10] Y. Khadouj Jelbaoui, L. El Menzhi, and A. Saad, "Diagnosis of induction motor failures using discrete wavelet transform of an auxiliary winding voltage," *Indonesian Journal of Electrical Engineering and Computer Science*, vol. 27, no. 3, p. 1231, Sep. 2022, doi: 10.11591/ijeecs.v27.i3.pp1231-1241.

[11] H. Henao, C. Demian, and G.-A. Capolino, "A frequency-domain detection of stator winding faults in induction machines using an external flux sensor," *IEEE Transactions on Industry Applications*, vol. 39, no. 5, pp. 1272–1279, Sep. 2003, doi: 10.1109/TIA.2003.816531.

[12] T. Samina, S. R. Iyer, and A. B. Beevi, "Rotor side control for improving the transient response of Doubly fed induction generator in wind power system," in *2017 International Conference on Technological Advancements in Power and Energy (TAP Energy)*, Dec. 2017, pp. 1–6. doi: 10.1109/TAPENERGY.2017.8397257.

[13] T. Assaf, H. Henao, and G.-A. Capolino, "Simplified axial flux spectrum method to detect incipient stator inter-turn short-circuits in induction machine," in *2004 IEEE International Symposium on Industrial Electronics*, 2004, pp. 815–819 vol. 2. doi: 10.1109/ISIE.2004.1571918.

[14] M. D. Negrea, "Electromagnetic Flux Monitoring for Detecting Faults in Electrical Machines," *Ph.D. Thesis*, 2006.

[15] V. Fireteanu, P. Lombard, and A. I. Constantin, "Detection of a short-circuit fault in the stator winding of induction motors through neighboring magnetic field harmonics," in *2014 International Conference on Electrical Machines (ICEM)*, Sep. 2014, pp. 1555–1561. doi: 10.1109/ICELMACH.2014.6960389.

[16] Zheng Liu, W. Cao, P.-H. Huang, G.-Y. Tian, and J. L. Kirtley, "Non-invasive winding fault detection for induction machines based on stray flux magnetic sensors," in *2016 IEEE Power and Energy Society General Meeting (PESGM)*, Jul. 2016, pp. 1–6. doi: 10.1109/PESGM.2016.7741486.

[17] P. C. M. Lamim Filho, R. Pederiva, and J. N. Brito, "Detection of stator winding faults in induction machines using flux and vibration analysis," *Mechanical Systems and Signal Processing*, vol. 42, no. 1–2, pp. 377–387, Jan. 2014, doi: 10.1016/j.ymssp.2013.08.033.

[18] Y. K. Jelbaoui, E. M. Lamiaà, and A. Saad, "Fault diagnosis of a squirrel cage induction motor fed by an inverter using lissajous curve of an auxiliary winding voltage," *Indonesian Journal of Electrical Engineering and Computer Science*, vol. 21, no. 3, p. 1299, Mar. 2021, doi: 10.11591/ijeecs.v21.i3.pp1299-1308.

[19] B. Sirisha and L. Yalakanti, "A mitigation technique for torque ripple in a brushless DC motor by controlled switching of small DC link capacitor," *Bulletin of Electrical Engineering and Informatics*, vol. 11, no. 2, pp. 1167–1176, Apr. 2022, doi: 10.11591/eei.v11i2.3408.

[20] R. Romary, R. Pusca, J. P. Lecointe, and J. F. Brudny, "Electrical machines fault diagnosis by stray flux analysis," in *2013 IEEE Workshop on Electrical Machines Design, Control and Diagnosis (WEMDCD)*, Mar. 2013, pp. 247–256. doi: 10.1109/WEMDCD.2013.6525184.

[21] V. D. Nhan, N. X. Bien, N. Q. Dich, and V. T. Ha, "Sliding-mode control design of a slotless self-bearing motor," *Bulletin of Electrical Engineering and Informatics*, vol. 11, no. 3, pp. 1297–1307, Jun. 2022, doi: 10.11591/eei.v11i3.3687.

[22] M. Gleissner, J. Haring, W. Wondrak, and M.-M. Bakran, "Analytical computation of normal and fault-tolerant active short circuit operation of anisotropic synchronous double star machines," in *2020 22nd European Conference on Power Electronics and Applications (EPE'20 ECCE Europe)*, Sep. 2020, pp. 1–10. doi: 10.23919/EPE20ECCEEurope43536.2020.9215753.

[23] Rahmaniar, A. Junaidi, Ganefri, A. K. Hamid, N. Jalinus, and J. Jama, "Modelling and simulation: An injection model approach to controlling dynamic stability based on unified power flow controller," *Journal of Theoretical and Applied Information Technology*, vol. 97, no. 20, pp. 2334–2345, 2019, doi: Modelling and simulation: An injection model approach to controlling dynamic stability based on unified power flow controller.

[24] M. Madark, A. Ba-razzouk, E. Abdelmounim, and M. El Malah, "Adaptive backstepping control of induction motor powered by photovoltaic generator," *International Journal of Electrical and Computer Engineering (IJECE)*, vol. 11, no. 4, p. 2842, Aug. 2021, doi: 10.11591/ijece.v11i4.pp2842-2855.

[25] A. Alabani, P. Ranjan, J. Jiang, L. Chen, I. Cotton, and V. Peesapati, "Electrical Characterization and Modeling of High Frequency Arcs for Higher Voltage Aerospace Systems," *IEEE Transactions on Transportation Electrification*, vol. 9, no. 3, pp. 4716–4725, Sep. 2023, doi: 10.1109/TTE.2023.3244776.

[26] H. S. Dakheel, Z. B. Abdullah, and S. W. Shneen, "Advanced optimal GA-PID controller for BLDC motor," *Bulletin of Electrical Engineering and Informatics*, vol. 12, no. 4, pp. 2077–2086, Aug. 2023, doi: 10.11591/eei.v12i4.4649.

[27] K. N. Gyftakis and A. J. M. Cardoso, "Reliable Detection of Stator Interturn Faults of Very Low Severity Level in Induction Motors," *IEEE Transactions on Industrial Electronics*, vol. 68, no. 4, pp. 3475–3484, 2021, doi: 10.1109/TIE.2020.2978710.

[28] Y. Park, H. Choi, J. Shin, J. Park, S. Bin Lee, and H. Jo, "Airgap flux based detection and classification of induction motor rotor and load defects during the starting transient," *IEEE Transactions on Industrial Electronics*, vol. 67, no. 12, pp. 10075–10084, 2020, doi: 10.1109/TIE.2019.2962470.

[29] P. A. Panagiotou, I. Arvanitakis, N. Lophitis, J. A. Antonino-Daviu, and K. N. Gyftakis, "A New Approach for Broken Rotor Bar Detection in Induction Motors Using Frequency Extraction in Stray Flux Signals," *IEEE Transactions on Industry Applications*, vol. 55, no. 4, pp. 3501–3511, 2019, doi: 10.1109/TIA.2019.2905803.

[30] M. N. Omar, M. M. Ismail, M. N. Ayob, and F. Arith, "Upgrading for overhead crane anti-sway method using variable frequency drive," *Bulletin of Electrical Engineering and Informatics*, vol. 11, no. 4, pp. 1837–1844, Aug. 2022, doi: 10.11591/eei.v11i4.3731.

[31] M. A. Mazzoletti, F. R. Gentile, P. D. Donolo, and G. R. Bossio, "Online detection of interturn short-circuit fault in induction motor based on 5th harmonic current tracking using Vold-Kalman filter," *International Journal of Electrical and Computer*

Engineering (IJECE), vol. 13, no. 4, p. 3593, Aug. 2023, doi: 10.11591/ijece.v13i4.pp3593-3605.

[32] D. Shi, P. J. Unsworth, and R. X. Gao, "Sensorless Speed Measurement of Induction Motor Using Hilbert Transform and Interpolated Fast Fourier Transform," *IEEE Transactions on Instrumentation and Measurement*, vol. 55, no. 1, pp. 290–299, Feb. 2006, doi: 10.1109/TIM.2005.860870.

[33] A. J. Ali, L. A. Khalaf, and A. H. Ahmed, "Modeling and simulation of a 3-ϕ induction motor based on two types of WFA," *International Journal of Electrical and Computer Engineering (IJECE)*, vol. 11, no. 2, pp. 110–1113, 2021, doi: 10.11591/ijece.v11i2.pp1105-1113.

BIOGRAPHIES OF AUTHORS

Rezi Delfianti 🆔 🔗 SC ⬡ was born in Padang, West Sumatera, on September 26th, 1996. She got Doctoral degree in the Electrical Engineering Department at Sepuluh Nopember Institute of Technology, Surabaya, Indonesia. She presently works as a lecturer in electrical engineering at the Faculty of Advanced Technology and Multidiscipline at Airlangga University Surabaya, Indonesia. Her research interests include power systems, solar energy stability, economics, applied machine learning, and data analytics for smart grids and smart cities, optimization business models, and mechanism design for incentivizing participation of electric vehicles and prosumers. She can be contacted at email: rezi.delfianti@ftmm.unair.ac.id.

Yusrizal Afif 🆔 🔗 SC ⬡ was born in Surabaya, East Java, Indonesia in 1992. He received Bachelor and Engineering degree in Electrical Engineering from Sepuluh Nopember Institute of Technology, Surabaya, Indonesia, in 2015. From 2015 to 2017 he worked as electrical engineer at Krakatau Engineering Co., Indonesia. He received Master Engineering degree in Electrical Engineering from Sepuluh Nopember Institute of Technology in 2019. He was joined Airlangga University in 2020 as lecturer. His research concentrates mainly on high voltage technology, apparatus characteristics, discharge phenomena and renewable energy. He can be contacted at email: yusrizal@ftmm.unair.ac.id.

Fidya Eka Prahesti 🆔 🔗 SC ⬡ was born on June 23, 1994 in Gresik. In 2012, she received a diploma's degree in electrical engineering from the faculty of industrial technology, ITS University, Indonesia, and in 2017, a bachelor's degree in electrical engineering from the faculty of electrical technology, ITS University. In 2020, she received her master degree in electrical engineering from the faculty of electrical Intelligent an informatics technology, ITS University. Currently working as a lecturer at the Faculty of Engineering, Nusantara PGRI University, Indonesia. Her research interests include high voltage, protection electrical system, and renewable energy. She can be contacted at email: feprahesti@gmail.com.

Bima Mustaqim 🆔 🔗 SC ⬡ is a magister student in the Educational Technology, Universitas Negeri Medan, Medan, Indonesia. He received his bachelor's degree in electrical engineering education from Universitas Negeri Medan, Indonesia, in 2018. He can be contacted at email: mustaqim.bima@gmail.com.

Bolas Boy Silalahi 🆔 🔗 SC ⬡ Born on the shores of Lake Toba, Laguboti, on the 16th December 1996. In 2014 continued studies in the Department of Electrical Engineering ITS by taking study programs Power System Engineering. His research concentrates mainly on high voltage technology and power systems simulation. He can be contacted at email: bolasboysilalahi@gmail.com.